Al-Nahrain Journal for Engineering Sciences

Al-Nahrain J. Eng. Sci. 29(1) 120-130, 2026
Original Article

Improvement and computational complexity reduction in estimating the direction of arrival using switched active switched parasitic antenna arrays for next- generation networks

Rabah Abduljabbar Jasem[1]●

1 Ph.D. Electrical Engineering

● *These authors contributed equally to this work*

DOI: http://doi.org/10.29194/NJES.29010120

Received: September 26, 2025 **Revised:** December 10, 2025 **Accepted:** December 28, 2025 **Published:** March 20, 2026

Abstract

This research studies the capabilities of antenna arrays known as switched active switched parasitic antennas (SASPA) in enhancing the direction of arrival (DOA) estimation of received signals. In these arrays, a single antenna element operates in an active state while the other antenna elements are parasitic at one time of measurement. In the next measurement time, a parasitic element is switched to an active state while the active element is switched to a parasitic state, and the procedure is quickly repeated for each array element. By a straightforward arrangement of SASPA measurements, a functional steering matrix can be produced without any unitary transformation. This steering matrix results from a real-valued matrix that contains the information on the DOAs of the received signals, multiplied by a vector that represents the mutual coupling. The advantages of this steering matrix contribute to obtaining high-resolution DOA estimation with considerably reduced processing time compared to the conventional antenna arrays where all antenna elements are in an active state. The simulations conducted in this study evidently demonstrate that the resolution of DOA estimation with SASPA arrays is considerably superior, irrespective of the array's compact size and the directions and proximity of received signals to each other. Additionally, other simulations in this work depict that the processing time for DOA estimation using SASPA arrays is significantly reduced (approximately one-third less on average) in comparison to traditional all-active antenna arrays.

Keywords: *Direction of Arrival Estimation, MUSIC Algorithm, Mutual Coupling, Switched Active Switched Parasitic Antenna Array.*

Corresponding author: Provide the corresponding author information and publisher here. E-mail address: rabah.aj@ntu.edu.iq

1. Introduction

Estimating Estimating the direction of arrival (DOA) of signals impinging on antenna arrays plays a vital role in data communications and signal processing, including MIMO systems [1], radar [2], wireless communications [3], IoT [4], and satellite communications [5]. Having precise knowledge of the angles of the incoming signals at the receiver allows the system to gain several advantages. One advantage is the secure transfer of data between the source and the recipient [6]. Moreover, estimating the DOAs can assist in suppressing interfering signals and noise [7]. Additionally, tracking multiple sources necessitates accurate identification of the origins of those sources simultaneously [6]. Precise DOA identification is also essential for decision-making applications, such as search and rescue missions, police efforts, and emergency response situations [6]. Consequently, DOA estimation leads to improved and more reliable functioning of the fundamental system under many conditions, such as a low signal-to-noise ratio (SNR) environments and others.

Several algorithms have been proposed for DOA estimation in the literature. Among them, the most recognized are MUSIC and ESPRIT. The MUSIC algorithm relies on the orthogonality between the subspace spanned by the columns of the steering matrix of the array and the noise subspace. The latter is calculated from the spectral decomposition of the covariance matrix of the array measurements when receiving the impinging signals. To achieve a very high-resolution DOA estimation, specific characteristics, such as directivity and switched radiation patterns offered by some types of antenna arrays, can be utilized. This calls for estimating the DOA of received signals with the aid of smart antenna arrays. In addition to playing a crucial role in determining the direction of received signals with very high resolution and avoiding unwanted signals [8, 9], the beneficial characteristics possessed by smart antenna arrays are capable of improving the

performance of multichannel systems (e.g., MIMO systems), where the usable power should be focused on the destination [10, 11].

Recently, antenna arrays with switched parasitic elements have been proposed for this purpose [11, 12]. The array consists of one element or more excited by the power supply when the array is in transmit mode, or connected to the load when the array is in receive mode. The other antenna elements are parasitic. By parasitic elements, it is meant that the terminals of these antennas are either short-circuited or connected to zero potential. These arrays fall into the category of smart antennas because they are flexible and fast in producing switched and steerable radiation patterns with a beam-formed main beam.

This study will explore the performance of an antenna array referred to as the switched active switched parasitic antenna (SASPA) array. This type of antenna array includes several antennas arranged in different configurations, such as a uniform linear array (ULA), a uniform circular array (UCA), and more. At any given moment, one element of the array is active, i.e., connected to the power supply, while the other elements are parasitic. In the subsequent moment, the element that was active is switched to a parasitic state, while a different element is switched to the active state. This process is performed rapidly and in a very short time. The outcome is the formation of a beamformed radiation pattern with a main beam directed in various directions. The radiation pattern beamforming and its directionality in different directions rely significantly on the mutual coupling among the array elements, particularly between the active component and the parasitic elements. Fast switching can be accomplished by incorporating electronic circuits controlled by PIN diodes in the antenna array circuitry. That is, the phase shifter, along with the related hardware and computer system used to control the RF signal feeding the array elements, is not required in SASPA arrays. Alternatively, simple hardware and software, lower cost, and a more compact array size are some advantages of SASPA arrays over phased array antennas. When used in receiving mode, the active element in a SASPA is connected to a load, while the other elements are parasitic. The most important advantage gained from a SASPA when used as a receiving array is the estimation of DOA with reduced computational complexity. A simple arrangement of the measurements of a SASPA-ULA array when receiving signals results in a useful steering matrix. The significance of this matrix lies in the product of a real-valued matrix and a column vector. The real-valued matrix depends on the DOAs of the received signals. The vector represents the mutual coupling in the array, which is usually represented by a matrix in the case of traditional (all-active) antenna arrays. This indicates lower computational complexity and reduced processing time in DOA estimation when a SASPA array is utilized. The benefits of real-valued DOA estimation are numerous, as recognized in the literature [1, 13-23]. Among these benefits are reduced calculations, enhanced system effectiveness, and greater resilience. Various techniques have been suggested in the literature to build real-valued antenna array data. Applying unitary transformations directly to the covariance matrix of the array measurements, which produces real values, is included in these techniques, as seen in [1, 13-16, 20, 21]. In [1, 15], a method is proposed to achieve a real-valued covariance matrix of an antenna array measurements by applying a unitary transformation matrix to the complex-valued covariance matrix in the presence of unknown mutual coupling. Before the transformation process, the covariance matrix is multiplied in advance and subsequently by a selection matrix that embeds the mutual coupling effect into the signal covariance matrix while keeping the array steering matrix free from mutual coupling. This is possible because of the inherent properties of the mutual coupling phenomenon, which is symmetric Toeplitz, and the assumption that no mutual coupling occurs among distant elements in the array. However, the signal subspace remains contaminated by the mutual coupling effect. Consequently, the effect of this phenomenon has not been accurately removed. Additionally, the elimination of mutual coupling in this study was not achieved due to the use of a unitary transformation on the measurements, as indicated in the research. The method used in [13] obtains real-valued signal and noise subspaces after performing Singular Value Decomposition (SVD) on the covariance matrix of the measurements from a receiving antenna array, following the application of a unitary transformation to this matrix. The weighted least squares approach is then used to estimate the DOAs by transforming the real-valued signal subspace obtained from the SVD back into a complex-valued subspace to fulfill the property of Linear Prediction (LP). However, the mutual coupling effect has not been considered in this work. In [14], the Khatri-Rao (KR) product is used to reduce the size of a real-valued covariance matrix converted from a complex-valued covariance matrix of a certain antenna array with all possible directions by applying a unitary transformation to this matrix. Additionally, the KR product allows the array to gain a virtual extension in size. Nevertheless, this study has also not taken into account the effect of mutual coupling. The study in [16] uses a series of unitary transformations on the covariance matrices constructed from the steering matrices of two subarrays of coprime arrays and their SVD decomposition. After considering and estimating the rotation matrices that rotate the steering matrices to the corresponding subspaces calculated from the SVD decomposition and using selection matrices, a diagonal matrix from which the DOAs can be estimated is obtained. The study in [20] exploits the unitary transformation for DOA estimation to reduce the extensive and lengthy complex computations required for processing the complex-valued covariance matrix of measurements of a ULA sensor array. The array is receiving a set of correlated and uncorrelated received signals. It is clear from the above studies that using unitary transformation, along with other proposed processing methods, to estimate the DOAs of the underlying signals might elevate the total error throughout the heavy computation procedure and increase the processing load. Furthermore, the idea of neglecting the mutual coupling effect between distant elements is impractical and may lead to incorrect DOA estimation, especially when the aperture of the antenna array is compact. Conversely, SASPA arrays offer a new, straightforward, simple, and effective approach to constructing a steering matrix with real-valued elements without any unitary transformation. The steering matrix of a SASPA array is formed

by a simple arrangement of the array dimensions, achieved by adding half of the measurements to the other half and subtracting one from the other during a single measurement instance. The outcome is a steering matrix formed by a real-valued matrix that depends on DOA, multiplied by a vector (not a matrix) that represents the effect of mutual coupling.

2. Data Model of an SASPA-ULA

Suppose that a set of P narrowband signals impinges on a Q-element SASPA-ULA array. The elements are half-wave dipole antennas spaced evenly along the x-axis, with a distance of r between each element, as illustrated in Fig. 1. Additionally, suppose that the number of elements, Q, is even.

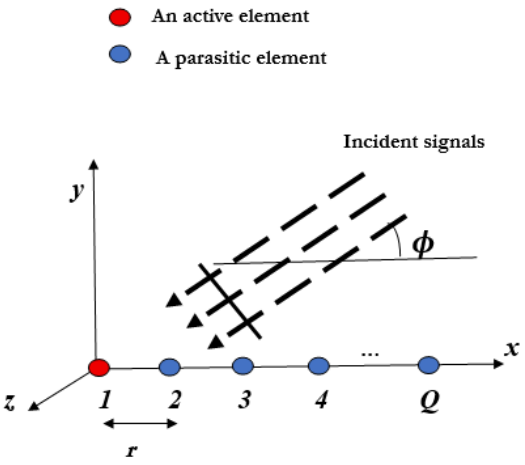

Figure 1. A Q-element SASPA-ULA array.

As previously noted, one element is switched to an active state (connected to the load) during a specific sub-snapshot, while the other elements remain parasitic. The array response to the received signals is detected as the measurement taken across the loaded terminals of the active element. This measurement comprises the voltage developed at the active element due to its induced current, plus the voltages coupled to the active element due to the short-circuit current induced in the parasitic elements. The measurement of the subsequent sub-snapshot is obtained when another element is switched to an active state and the previously active element is returned to a parasitic state. Thus, a frame of Q sub-measurements will be achieved within one measurement snapshot. As previously pointed out, the movement from one sub-measurement to the next one is carried out using PIN diodes in the circuitry of each antenna in the array. Neglecting the effect of the transition time between successive sub-measurements by assuming the switching time of PIN diodes is very small compared to the transition time between snapshots, the nondirectional measurement when the element q is active in a SASPA-ULA receiving one signal $s(t)$ can be expressed as:

$$\mathrm{x}^{(q)}(t) = \mathrm{M}^{(q)}\mathrm{a}\,(\phi)s(t) \quad \cdots (1)$$

Where $\mathrm{x}^{(q)}(t) = [0 \;\; 0 \;\; \mathrm{x}_q(t) \;\; 0 \;\cdots 0]^T \in \mathbb{C}^{Q\times 1}$. M is the mutual coupling matrix (MCM) with a Toeplitz structure, and has the following form:

$$\mathrm{M} = \begin{bmatrix} m_{11} & m_{12} & m_{13} & \cdots & m_{1Q} \\ m_{21} & m_{22} & m_{23} & \cdots & m_{2Q} \\ m_{31} & m_{32} & m_{33} & \cdots & m_{3Q} \\ \vdots & \vdots & \vdots & \ddots & \vdots \\ m_{Q1} & m_{Q2} & m_{Q3} & \cdots & m_{QQ} \end{bmatrix} \in \mathbb{C}^{Q\times Q} \quad \ldots(2)$$

The unit of the entries of M depends on the model used to interpret the mutual coupling phenomenon in antenna arrays. They will be unitless if the mutual coupling model relates the coupled voltage measurements to uncoupled voltages. If the model relates the coupled currents to the uncoupled voltages, the units of the entries will be in ohms. For the case of a SASPA-ULA, M will have the following structure when element q is active:

$$\mathrm{M}^{(q)} = \begin{bmatrix} 0 & 0 & 0 & \cdots & 0 \\ 0 & 0 & 0 & \cdots & 0 \\ m_{q1} & m_{q2} & m_{q3} & \cdots & m_{qQ} \\ \vdots & \vdots & \vdots & \ddots & \vdots \\ 0 & 0 & 0 & \cdots & 0 \end{bmatrix} \quad \ldots(3)$$

The elements of the steering vector, $\mathrm{a}\,(\phi)$, represent the response of the array antennas to the received signals. If the signals are incident on the array in the *x-y* plane and the gain of the antenna elements is unity due to the half-wave dipole assumption [24], then $\mathrm{a}\,(\phi)$ of a ULA array with its first element placed at the origin (see Fig.1) has the following entries:

$$\mathrm{a}\,(\phi) = [1 \quad e^{j\alpha} \quad \ldots \quad e^{j(Q-1)\alpha}]^T \in \mathbb{C}^{Q\times 1} \quad \ldots (4)$$

Where $\alpha = krcos\phi$. $k = 2\pi/\lambda$ is the wave number, and λ is the wavelength of the received signals. Note that the unit of $e^{jq\alpha}$ is radians. Eq. (1) indicates that the measurement $\mathrm{x}^{(q)}(t)$ is a zero vector with only one nonzero entry, which corresponds to the measurement at the active element. Thus, this measurement refers to the element space. As a SASPA-ULA provides inherent directivity, the measurement in eq. (1) should represent the beam space measurement, i.e., a single value. To obtain this beam space measurement, $\mathrm{x}^{(q)}(t)$ should be pre-multiplied by $\mathrm{a}^H(\phi)$ [25], where H is the Hermitian operation. Therefore, the beam space measurement when element q is active is given by:

$$\mathrm{x}_{BS}^{(q)}(t) = \mathrm{a}^H(\phi)\mathrm{M}^{(q)}\mathrm{a}\,(\phi)s(t) = e^{-j(q-1)\alpha}\mathrm{m}^{(q)^T}\mathrm{a}\,(\phi)s(t) \quad \in \mathbb{C}^{1\times 1} \quad \ldots (5)$$

Where $\mathbf{m}^{(q)^T}$ is the qth row of the matrix $\mathbf{M}^{(q)}$. Notice that making one element active in a SASPA-ULA will add an additional phase shift, $e^{-j(q-1)\alpha}$ to the received signal. This added phase shift will play a significant role in enhancing the estimation of the DOA of received signals using SASPA arrays. When P signals are received by the array, the measurement $\mathrm{x}_{BS}^{(q)}(t)$ will be the superposition of the responses to these signals, i.e.,

$$\begin{aligned}\mathrm{x}_{BS}^{(q)}(t) = {} & e^{-j(q-1)\alpha_1}\mathbf{m}^{(q)^T}\mathbf{a}\,(\phi_1)s_1(t) + \\ & e^{-j(q-1)\alpha_2}\mathbf{m}^{(q)^T}\mathbf{a}\,(\phi_2)s_2(t) + \ldots + \\ & e^{-j(q-1)\alpha_P}\mathbf{m}^{(q)^T}\mathbf{a}\,(\phi_P)s_P(t) \\ = {} & \mathbf{m}^{(q)^T}\mathbf{A}(\phi)\boldsymbol{\mathcal{B}}^{q-1}\mathbf{s}(t) \quad \cdots (6)\end{aligned}$$

Where $\mathbf{A}(\phi)$ is the steering matrix, defined as:

$$\mathbf{A}(\phi) = \begin{bmatrix} 1 & 1 & \cdots & 1 \\ e^{j\alpha_1} & e^{j\alpha_p} & \ldots & e^{j\alpha_P} \\ e^{j2\alpha_1} & e^{j2\alpha_p} & \ldots & e^{j2\alpha_P} \\ \vdots & \vdots & \ddots & \vdots \\ e^{j(Q-1)\alpha_1} & e^{j(Q-1)\alpha_p} & \ldots & e^{j(Q-1)\alpha_P} \end{bmatrix} \in \mathbb{C}^{Q\times P} \quad (7)$$

$$\boldsymbol{\mathcal{B}}^{q-1} = \text{diag}\begin{bmatrix} e^{-j(q-1)\alpha_1} & & \\ & e^{-j(q-1)\alpha_2} & \\ & \dots & \\ & & e^{-j(q-1)\alpha_P} \end{bmatrix}^T \in \mathbb{C}^{P\times P} \cdots(8)$$

$$\mathbf{s}(t) = [\mathrm{s}_1(t) \quad \mathrm{s}_2(t) \quad \cdots \quad \mathrm{s}_P(t)]^T \in \mathbb{C}^{P\times 1} \quad \cdots(9)$$

The noisy measurement of one snapshot is the result of gathering the frames of Q sub measurements as follows:

$$\mathbf{x}_{\boldsymbol{SASPA-ULA}}(t) = \left[\mathrm{x}_{BS}^{(1)}(t) \quad \mathrm{x}_{BS}^{(2)}(t) \quad \cdots \quad \mathrm{x}_{BS}^{(Q)}(t)\right]^T = \begin{bmatrix} \mathbf{m}^{(1)^T}\mathbf{A}(\phi) \\ \mathbf{m}^{(2)^T}\mathbf{A}(\phi)\boldsymbol{\mathcal{B}} \\ \mathbf{m}^{(3)^T}\mathbf{A}(\phi)\boldsymbol{\mathcal{B}}^2 \\ \vdots \\ \mathbf{m}^{(Q)^T}\mathbf{A}(\phi)\boldsymbol{\mathcal{B}}^{Q-1} \end{bmatrix}\mathbf{s}(t) + \begin{bmatrix} \mathrm{n}^{(1)}(t) \\ \mathrm{n}^{(2)}(t) \\ \mathrm{n}^{(3)}(t) \\ \vdots \\ \mathrm{n}^{(Q)}(t) \end{bmatrix} \cdots(10)$$

The noise, $\mathrm{n}^{(q)}(t)$, in eq. (10) is the noise that contaminates the measurement at the active element *q*. In this work, it is assumed that this noise is Additive White Gaussian Noise (AWGN) with a normal distribution. Additionally, this noise is assumed to have a zero mean and a power of σ^2. Furthermore, it is assumed that this noise is uncorrelated with the received signals. In general, when the number of elements in an antenna array is even, each row of the matrix $\mathbf{M}$ can be written as:

$$\mathbf{m}^{(Q+1-q)^T} = \mathbf{m}^{(q)^T}\boldsymbol{\Pi} \quad \cdots(11)$$

Where $\boldsymbol{\Pi}$ is a $Q \times Q$ exchange matrix, and is defined as:

$$\boldsymbol{\Pi} = \begin{bmatrix} 0 & 0 & . & . & . & 1 \\ 0 & . & . & . & 1 & 0 \\ . & . & . & 1 & . & 0 \\ . & . & 1 & . & . & . \\ . & . & . & . & . & 0 \\ 1 & . & . & . & 0 & 0 \end{bmatrix} \quad \cdots(12)$$

With ones on the antidiagonal and zeros elsewhere. Thus, the system in eq. (10) can be rewritten as:

$$\mathbf{x}_{\boldsymbol{SASPA-ULA}}(t) = \begin{bmatrix} \mathrm{x}_{BS}{}^{(1)}(t) \\ \mathrm{x}_{BS}{}^{(2)}(t) \\ . \\ . \\ \mathrm{x}_{BS}{}^{(Q/2)}(t) \\ \mathrm{x}_{BS}{}^{(Q/2+1)}(t) \\ . \\ . \\ \mathrm{x}_{BS}{}^{(Q)}(t) \end{bmatrix} = \begin{bmatrix} \mathbf{m}^{(1)^T}\mathbf{A}^{(1)}(\phi) \\ \mathbf{m}^{(2)^T}\mathbf{A}^{(2)}(\phi) \\ . \\ . \\ \mathbf{m}^{(Q/2)^T}\mathbf{A}^{(Q/2)}(\phi) \\ \mathbf{m}^{(Q/2+1)^T}\mathbf{A}^{(Q/2+1)}(\phi) \\ . \\ . \\ \mathbf{m}^{(Q)^T}\mathbf{A}^{(Q)}(\phi) \end{bmatrix}\mathbf{s}(t) + \begin{bmatrix} \mathrm{n}^{(1)}(t) \\ \mathrm{n}^{(2)}(t) \\ . \\ . \\ \mathrm{n}^{(Q/2)}(t) \\ \mathrm{n}^{(Q/2+1)}(t) \\ . \\ . \\ \mathrm{n}^{(Q)}(t) \end{bmatrix} \cdots(13)$$

Where $\mathbf{A}^{(q)}(\phi) = \mathbf{A}(\phi)\boldsymbol{\mathcal{B}}^{q-1}$ is the steering matrix of a SASPA-ULA when element *q* is active. Using eq. (11) in eq. (13) yields:

$$\mathbf{x}_{\boldsymbol{SASPA-ULA}}(t) = \begin{bmatrix} \mathrm{x}_{BS}{}^{(1)}(t) \\ \mathrm{x}_{BS}{}^{(2)}(t) \\ . \\ . \\ \mathrm{x}_{BS}{}^{(Q/2)}(t) \\ \mathrm{x}_{BS}{}^{(Q/2+1)}(t) \\ . \\ . \\ \mathrm{x}_{BS}{}^{(Q)}(t) \end{bmatrix} = \begin{bmatrix} \mathbf{m}^{(1)^T}\mathbf{A}^{(1)}(\phi) \\ \mathbf{m}^{(2)^T}\mathbf{A}^{(2)}(\phi) \\ . \\ . \\ \mathbf{m}^{(Q/2)^T}\mathbf{A}^{(Q/2)}(\phi) \\ \mathbf{m}^{(Q/2)^T}\boldsymbol{\Pi}\mathbf{A}^{(Q/2+1)}(\phi) \\ . \\ \mathbf{m}^{(2)^T}\boldsymbol{\Pi}\mathbf{A}^{(Q-1)}(\phi) \\ \mathbf{m}^{(1)^T}\boldsymbol{\Pi}\mathbf{A}^{(Q)}(\phi) \end{bmatrix}\mathbf{s}(t) + \begin{bmatrix} \mathrm{n}^{(1)}(t) \\ \mathrm{n}^{(2)}(t) \\ . \\ . \\ \mathrm{n}^{(Q/2)}(t) \\ \mathrm{n}^{(Q/2+1)}(t) \\ . \\ . \\ \mathrm{n}^{(Q-1)}(t) \\ \mathrm{n}^{(Q)}(t) \end{bmatrix} \cdots(14)$$

Now, pre-multiplying the steering vector $\boldsymbol{a}^{(Q+1-q)}(\phi)$ by the exchange matrix $\boldsymbol{\Pi}$ yields the conjugate of $\boldsymbol{a}^{(q)}(\phi)$, i.e.:

$$\boldsymbol{\Pi}\boldsymbol{a}^{(Q+1-q)}(\phi) = \boldsymbol{a}^{(q)^*}(\phi) \quad \cdots(15)$$

Applying eq. (15) to eq. (14) yields:

$$\mathbf{x}_{\boldsymbol{SASPA-ULA}}(t) = \begin{bmatrix} \mathrm{x}_{BS}{}^{(1)}(t) \\ \mathrm{x}_{BS}{}^{(2)}(t) \\ . \\ . \\ \mathrm{x}_{BS}{}^{(Q/2)}(t) \\ \mathrm{x}_{BS}{}^{(Q/2+1)}(t) \\ . \\ . \\ \mathrm{x}_{BS}{}^{(Q)}(t) \end{bmatrix} = \begin{bmatrix} \mathbf{m}^{(1)^T}\mathbf{A}^{(1)}(\phi) \\ \mathbf{m}^{(2)^T}\mathbf{A}^{(2)}(\phi) \\ . \\ . \\ \mathbf{m}^{(Q/2)^T}\mathbf{A}^{(Q/2)}(\phi) \\ \mathbf{m}^{(Q/2)^T}\mathbf{A}^{(Q/2)^\star}(\phi) \\ . \\ \mathbf{m}^{(2)^T}\mathbf{A}^{(2)^\star}(\phi) \\ \mathbf{m}^{(1)^T}\mathbf{A}^{(1)^\star}(\phi) \end{bmatrix}\mathbf{s}(t) + \begin{bmatrix} n^{(1)}(t) \\ n^{(2)}(t) \\ . \\ . \\ n^{(Q/2)}(t) \\ n^{(Q/2+1)}(t) \\ . \\ . \\ n^{(Q-1)}(t) \\ n^{(Q)}(t) \end{bmatrix} \cdots(16)$$

Adding the first Q/2 measurements to the remaining flipped upside-down Q/2 measurements in eq. (16) produces a new Q/2 measurement column vector, which is defined as:

$$\mathbf{y}_{\boldsymbol{SASPA-ULA,1}}(t) = \begin{bmatrix} \mathrm{x}_{BS}{}^{(1)}(t) + \mathrm{x}_{BS}{}^{(Q)}(t) \\ \mathrm{x}_{BS}{}^{(2)}(t) + \mathrm{x}_{BS}{}^{(Q-1)}(t) \\ . \\ \mathrm{x}_{BS}{}^{(q)}(t) + \mathrm{x}_{BS}{}^{(Q+1-q)}(t) \\ . \\ . \\ \mathrm{x}_{BS}{}^{\left(\frac{Q}{2}\right)}(t) + \mathrm{x}_{BS}{}^{\left(\frac{Q}{2}+1\right)}(t) \end{bmatrix}$$

$$= \begin{bmatrix} \mathbf{m}^{(1)^T}\left(\mathbf{A}^{(1)}(\phi)+\mathbf{A}^{(1)^\star}(\phi)\right) \\ \mathbf{m}^{(2)^T}\left(\mathbf{A}^{(2)}(\phi)+\mathbf{A}^{(2)^\star}(\phi)\right) \\ . \\ \mathbf{m}^{(q)^T}\left(\mathbf{A}^{(q)}(\phi)+\mathbf{A}^{(q)^\star}(\phi)\right) \\ . \\ . \\ \mathbf{m}^{\left(\frac{Q}{2}\right)^T}\left(\mathbf{A}^{\left(\frac{Q}{2}\right)}(\phi)+\mathbf{A}^{\left(\frac{Q}{2}\right)^\star}(\phi)\right) \end{bmatrix} \mathbf{s}(t) + \begin{bmatrix} \left(n^{(1)}(t)+n^{(Q)}(t)\right) \\ \left(n^{(2)}(t)+n^{(Q-1)}(t)\right) \\ . \\ \left(n^{(q)}(t)+n^{(Q+1-q)}(t)\right) \\ . \\ . \\ \left(n^{\left(\frac{Q}{2}\right)}(t)+n^{\left(\frac{Q}{2}+1\right)}(t)\right) \end{bmatrix}$$

$$\therefore \mathbf{y_{SASPA-ULA,1}}(t) = \begin{bmatrix} 2\mathbf{m}^{(1)^T}\left(Re\left(\mathbf{A}^{(1)}(\phi)\right)\right) \\ 2\mathbf{m}^{(2)^T}\left(Re\left(\mathbf{A}^{(2)}(\phi)\right)\right) \\ . \\ 2\mathbf{m}^{(q)^T}\left(Re\left(\mathbf{A}^{(q)}(\phi)\right)\right) \\ . \\ 2\mathbf{m}^{\left(\frac{Q}{2}\right)^T}\left(Re\left(\mathbf{A}^{\left(\frac{Q}{2}\right)}(\phi)\right)\right) \end{bmatrix} \mathbf{s}(t) + \begin{bmatrix} \bar{n}^{(1)}(t) \\ \bar{n}^{(2)}(t) \\ . \\ \bar{n}^{(q)}(t) \\ . \\ \bar{n}^{\left(\frac{Q}{2}\right)}(t) \end{bmatrix}$$

or

$$\mathbf{y_{SASPA-ULA,1}}(t) = \mathbf{G}_1(\phi)\mathbf{s}(t) + \bar{\mathbf{n}}(t) \qquad \cdots (17)$$

In eq. (17), $Re\left(\mathbf{A}^{(q)}(\phi)\right)$ is the real part of the steering matrix $\mathbf{A}^{(q)}(\phi)$. The formula for $Re\left(\mathbf{A}^{(q)}(\phi)\right)$, when a single signal is received by the array, is:

$$Re\left(\boldsymbol{a}(\phi_p)^{(q)}\right) = \left[cos\left((-q+1)\alpha_p\right) \quad cos\left((-q+2)\alpha_p\right) \ \ldots \ cos\left((-q+Q)\alpha_p\right)\right]^T = \mathbf{g_1}(\phi_p)^{(q)} \qquad \cdots (18)$$

Another Q/2 new measurement column vector can be obtained by subtracting the remaining flipped upside-down Q/2 measurements from the first Q/2 measurements of eq. (16), i.e.:

$$\mathbf{y_{SASPA-ULA,2}}(t) = \begin{bmatrix} \mathrm{x}_{BS}{}^{(1)}(t) - \mathrm{x}_{BS}{}^{(Q)}(t) \\ \mathrm{x}_{BS}{}^{(2)}(t) - \mathrm{x}_{BS}{}^{(Q-1)}(t) \\ . \\ \mathrm{x}_{BS}{}^{(q)}(t) - \mathrm{x}_{BS}{}^{(Q+1-q)}(t) \\ . \\ . \\ \mathrm{x}_{BS}{}^{\left(\frac{Q}{2}\right)}(t) - \mathrm{x}_{BS}{}^{\left(\frac{Q}{2}+1\right)}(t) \end{bmatrix}$$

$$= \begin{bmatrix} \mathbf{m}^{(1)^T}\left(\mathbf{A}^{(1)}(\phi)-\mathbf{A}^{(1)^\star}(\phi)\right) \\ \mathbf{m}^{(2)^T}\left(\mathbf{A}^{(2)}(\phi)-\mathbf{A}^{(2)^\star}(\phi)\right) \\ . \\ \mathbf{m}^{(q)^T}\left(\mathbf{A}^{(q)}(\phi)-\mathbf{A}^{(q)^\star}(\phi)\right) \\ . \\ . \\ \mathbf{m}^{\left(\frac{Q}{2}\right)^T}\left(\mathbf{A}^{\left(\frac{Q}{2}\right)}(\phi)-\mathbf{A}^{\left(\frac{Q}{2}\right)^\star}(\phi)\right) \end{bmatrix} \mathbf{s}(t) + \begin{bmatrix} \left(n^{(1)}(t)-n^{(Q)}(t)\right) \\ \left(n^{(2)}(t)-n^{(Q-1)}(t)\right) \\ . \\ \left(n^{(q)}(t)-n^{(Q+1-q)}(t)\right) \\ . \\ . \\ \left(n^{\left(\frac{Q}{2}\right)}(t)-n^{\left(\frac{Q}{2}+1\right)}(t)\right) \end{bmatrix}$$

$$\therefore \mathbf{y_{SASPA-ULA,2}}(t) = \begin{bmatrix} 2\mathbf{m}^{(1)^T}\left(Im\left(\mathbf{A}^{(1)}(\phi)\right)\right) \\ 2\mathbf{m}^{(2)^T}\left(Im\left(\mathbf{A}^{(2)}(\phi)\right)\right) \\ . \\ 2\mathbf{m}^{(q)^T}\left(Im\left(\mathbf{A}^{(q)}(\phi)\right)\right) \\ . \\ 2\mathbf{m}^{\left(\frac{Q}{2}\right)^T}\left(Im\left(\mathbf{A}^{\left(\frac{Q}{2}\right)}(\phi)\right)\right) \end{bmatrix} \mathbf{s}(t) + \begin{bmatrix} \bar{\bar{n}}^{(1)}(t) \\ \bar{\bar{n}}^{(2)}(t) \\ . \\ \bar{\bar{n}}^{(q)}(t) \\ . \\ \bar{\bar{n}}^{\left(\frac{Q}{2}\right)}(t) \end{bmatrix}$$

or

$$\mathbf{y_{SASPA-ULA,2}}(t) = \mathbf{G}_2(\phi)\mathbf{s}(t) + \bar{\bar{\mathbf{n}}}(t) \qquad \cdots (19)$$

With $Im\left(\mathbf{A}^{(q)}(\phi)\right)$ as the imaginary part of $\mathbf{A}^{(q)}(\phi)$, and:

$$Im\left(\boldsymbol{a}(\phi_p)^{(q)}\right) = \left[sin\left((-q+1)\alpha_p\right) \quad sin\left((-q+2)\alpha_p\right) \ \ldots sin\left((-q+Q)\alpha_p\right)\right]^T = \mathbf{g_2}(\phi_p)^{(q)} \qquad \cdots (20)$$

Notice that eq. (19) was multiplied by *-j* to eliminate the factor *j* associated with $Im\left(\mathbf{A}^{(q)}(\phi)\right)$. This exchanges the real and imaginary parts of $\mathbf{y_{SASPA-ULA,2}}(t)$ with no loss of DOA information. Additionally, it has no effect on the complex value of the noise. Furthermore, summing two AWGN noises or subtracting one from the other results in another AWGN noise with a normal distribution [26, 27]. When a single signal is received, each element in the matrices $\mathbf{G_1}(\phi)$ and $\mathbf{G_2}(\phi)$ can be rewritten, respectively, as:

$$2\mathbf{m}^{(q)^T} Re\left(\mathbf{a}^{(q)}(\phi_p)\right) = 2\mathbf{g_1}(\phi_p)^{(q)^T}\mathbf{m}^{(q)} \qquad \cdots (21)$$

$$2\mathbf{m}^{(q)^T} Im\left(\mathbf{a}^{(q)}(\phi_p)\right) = 2\mathbf{g_2}(\phi_p)^{(q)^T}\mathbf{m}^{(q)} \qquad \cdots (22)$$

Thus, the system in eq. (16) can be updated as follows:

$$\mathbf{y}(t)=\begin{bmatrix}\mathbf{y}_{SASPA-ULA,1}(t)\\ \mathbf{y}_{SASPA-ULA,2}(t)\end{bmatrix}=\begin{bmatrix}\mathbf{G}_1(\phi)\\ \mathbf{G}_2(\phi)\end{bmatrix}\mathbf{s}(t)+\begin{bmatrix}\bar{\mathbf{n}}(t)\\ \bar{\bar{\mathbf{n}}}(t)\end{bmatrix}$$

or $\mathbf{y}(t)=\mathbf{G}(\phi)\mathbf{s}(t)+\mathbf{n}(t)$ ⋯(23)

Furthermore, the matrix $\mathbf{G}(\phi_p)$ can be rewritten as:

$$\mathbf{G}(\phi_p)=\mathbf{K}(\phi_p)\mathbf{m}^{(1)}=\left(\mathbf{K_1}(\phi_p)\odot\mathbf{K_2}\right)\mathbf{m}^{(1)}$$
$$p=1,2,\ldots\ldots,P \qquad \cdots (24)$$

With $\odot$ being the Hadamard (element-by-element) matrix product. Notice that the mutual coupling is represented by the vector $\mathbf{m}^{(1)}$only. The matrix $\mathbf{K_1}(\phi_p)$ is as follows:

$$\mathbf{K_1}(\phi_p)=2\begin{bmatrix}\mathbf{g_1}(\phi_p)^{(1)^T}\\ \vdots\\ \mathbf{g_1}(\phi_p)^{(1)^T}\\ \mathbf{g_2}(\phi_p)^{(1)^T}\\ \vdots\\ \mathbf{g_2}(\phi_p)^{(1)^T}\end{bmatrix}\in\mathbb{R}^{Q\times Q} \qquad \cdots (25)$$

The structure of the matrix $\mathbf{K_2}=\begin{bmatrix}\mathbf{K_{21}}\\ \mathbf{K_{22}}\end{bmatrix}\in\mathbb{Z}^{Q\times Q}$ is as follows:

$$\mathbf{K_{21}}=\begin{bmatrix}1&1&1&1&.&.&.&.&1&1\\ 1&2&1&1&.&.&.&.&1&0\\ 1&2&2&1&.&.&.&1&0&0\\ .&.&.&.&.&.&.&.&.&.\\ 1&2&2&2&2&1&0&0&0&0\end{bmatrix}\begin{matrix}\\ \\ \\ \\ Q/2-1\end{matrix}$$
Q/2 Q/2-1 ⋯ (26)

$$\mathbf{K_{22}}=\begin{bmatrix}1&1&1&1&.&.&.&.&1&1\\ 0&0&1&1&.&.&.&.&1&0\\ 0&0&0&1&.&.&.&1&0&0\\ .&.&.&.&.&.&.&.&.&.\\ 0&0&0&0&0&1&0&0&0&0\end{bmatrix}\begin{matrix}\\ \\ \\ \\ Q/2-1\end{matrix}$$
Q/2 Q/2-1 ⋯ (27)

Thus, eq. (23) will finally be written as:

$$\mathbf{y}(t)=\left[\mathbf{K}(\phi_1)\mathbf{m}^{(1)}\ \ \mathbf{K}(\phi_2)\mathbf{m}^{(1)}\ \ldots\ \mathbf{K}(\phi_P)\mathbf{m}^{(1)}\right]\mathbf{s}(t)+\mathbf{n}(t)$$
$$=\left[\mathbf{K}(\phi_1)\ \ \mathbf{K}(\phi_2)\ \ldots\ \mathbf{K}(\phi_P)\right]\left(\boldsymbol{I}_P\otimes\mathbf{m}^{(1)}\right)\mathbf{s}(t)+\mathbf{n}(t)$$
$$=\boldsymbol{\Gamma}(\phi)\mathbf{Z}\mathbf{s}(t)+\mathbf{n}(t)=\mathbf{A}_{SASPA-ULA}(\phi)\mathbf{s}(t)+\mathbf{n}(t) \qquad \cdots (28)$$

with

$$\mathbf{A}_{SASPA-ULA}(\phi)=\boldsymbol{\Gamma}(\phi)\mathbf{Z} \qquad \cdots (29)$$

Where $\boldsymbol{\Gamma}(\phi)=\left[\mathbf{K}(\phi_1)\ \ \mathbf{K}(\phi_2)\ \ldots\ \mathbf{K}(\phi_P)\right]\in\mathbb{R}^{Q\times(PQ)}$ and $\mathbf{Z}=\left(\boldsymbol{I}_P\otimes\mathbf{m}^{(1)}\right)\in\mathbb{C}^{PQ\times P}$.

The operation $\otimes$ denotes the Kronecker matrix product. The matrix $\boldsymbol{\Gamma}(\phi)$ is full row rank, i.e., $\mathrm{rk}\left(\boldsymbol{\Gamma}(\phi)\right)=\mathrm{Q}$ if the received signals are totally uncorrelated, while the matrix $\mathbf{Z}$ is full column rank with $\mathrm{rk}(\mathbf{Z})=P$.

The data model in eq. (28) reveals that the steering matrix of a SASPA-ULA, i.e., $\mathbf{A}_{SASPA-ULA}(\phi)=\boldsymbol{\Gamma}(\phi)\mathbf{Z}$ is the product of two matrices. The first one, $\boldsymbol{\Gamma}(\phi)$, is a ***real-valued*** matrix and depends on the DOAs of the incoming signals. The other matrix, $\mathbf{Z}$, represents the mutual coupling effect in the array. However, this matrix is expressed in terms of one vector, $\mathbf{m}^{(1)}$, rather than the matrix $\mathbf{M}$. This means that when the data is processed for DOA estimation, a significant reduction in computational complexity can be achieved. The accumulated computational errors are also decreased. As a result, faster data processing and reduced power consumption can be achieved, i.e., an improvement in system efficiency. These advantages are crucial for wireless communications, specifically when taking place in dense urban areas where the signal-to-noise (SNR) ratio is very low.

The covariance matrix of the measurements, $\mathbf{D}\in\mathbb{C}^{\boldsymbol{Q\times Q}}$, is obtained from:

$$\mathbf{D}=E(\mathbf{y}(t)\mathbf{y}(t)^H)$$
$$=\mathbf{A}_{SASPA-ULA}(\phi)E(\mathbf{s}(t)\mathbf{s}(t)^H)\mathbf{A}_{SASPA-ULA}(\phi)^H$$
$$+E(\mathbf{n}(t)\mathbf{n}(t)^H)$$
$$=\left[\mathbf{K}(\phi_1)\ \ \mathbf{K}(\phi_2)\ \ldots\ \mathbf{K}(\phi_P)\right]E\left(\left(\mathbf{s}(t)\otimes\mathbf{m}^{(1)}\right)\left(\mathbf{s}(t)\otimes\mathbf{m}^{(1)}\right)^H\right)\begin{bmatrix}\mathbf{K}^T(\phi_1)\\ \mathbf{K}^T(\phi_2)\\ .\\ .\\ \mathbf{K}^T(\phi_P)\end{bmatrix}+\sigma^2\boldsymbol{I}_N$$

Or

$$\mathbf{D}=E(\mathbf{y}(t)\mathbf{y}(t)^H)$$
$$=\boldsymbol{\Gamma}(\phi)\left(\mathbf{s}(t)\mathbf{s}(t)^H\otimes\mathbf{m}^{(1)}\mathbf{m}^{(1)^H}\right)\boldsymbol{\Gamma}(\phi)^T+\sigma^2\boldsymbol{I}_Q$$

i.e.,

$$\mathbf{D}=E(\mathbf{y}(t)\mathbf{y}(t)^H)$$
$$=\boldsymbol{\Gamma}(\phi)\left(\mathbf{S}\otimes\mathbf{M}^{(1)}\right)\boldsymbol{\Gamma}(\phi)^T+\sigma^2\boldsymbol{I}_Q \qquad \cdots (30)$$

Where $\mathbf{M}^{(1)}=\mathbf{m}^{(1)}\mathbf{m}^{(1)^H}$. In processing eq. (30), the expectation operator $E(.)$ is statistically calculated for the random variables only: $\mathbf{s}(t)$ and $\mathbf{n}(t)$. Thus, $E\left(\left(\mathbf{s}(t)\otimes\mathbf{m}^{(1)}\right)\left(\mathbf{s}(t)\otimes\mathbf{m}^{(1)}\right)^H\right)=\left(\mathbf{S}\otimes\mathbf{M}^{(1)}\right)$ [28], and $E(\mathbf{n}(t)\mathbf{n}(t)^H)=\sigma^2\mathbf{I_Q}$ assuming these variables follow a normal distribution and the noise has a zero mean value. The matrix $\mathbf{S}$ is diagonal with the signal power on its diagonal when the received signals are uncorrelated with each other. Additionally, the received signals and the noise are assumed to be non-coherent; accordingly, the cross-product terms vanish.

The components of the RHS of the system in eq. (30) are real-valued, with the exception of $\mathbf{M}^{(1)}$. To tackle the existence of only one element with complex values, i.e., $\mathbf{M}^{(1)}$, the measurement $\mathbf{y}(t)$ in eq. (28) can be added to its conjugate, i.e., $\mathbf{y}(t)^*$. Thus, eq. (28) and eq. (30) become, respectively:

$$\mathbf{y}_{rv}(t)=(\mathbf{y}(t)+\mathbf{y}(t)^*)/2$$
$$=\boldsymbol{\Gamma}(\phi)\mathrm{real}((\mathbf{Z})\mathbf{s}(t))+\mathrm{real}(\mathbf{n}(t)) \qquad \cdots (31)$$

$$\mathbf{D}_{rv}=\boldsymbol{\Gamma}(\phi)(\mathrm{real}(\mathbf{Z}\mathbf{s}(t))(\mathrm{real}(\mathbf{Z}\mathbf{s}(t)))^T)\boldsymbol{\Gamma}(\phi)^T$$
$$+\sigma_{rv}^2\boldsymbol{I}_Q \qquad \cdots (32)$$

Where the subscript rv stands for 'real-valued'. Note that the accumulated noise is still normally distributed. That is, the expectation, $E(\mathrm{real}(\mathbf{n}(t))\mathrm{real}(\mathbf{n}(\boldsymbol{t})^{\boldsymbol{H}}))=\sigma_{rv}^2\boldsymbol{I}_Q$, is still valid. Practically, the matrices $\mathbf{D}$ and $\mathbf{D}_{rv}$ can be calculated from:

$$\breve{\mathbf{D}} = \frac{1}{C}\sum_{c=1}^{C} \mathbf{y}(t_c)\mathbf{y}(t_c)^H \quad \cdots(33)$$

$$\breve{\mathbf{D}}_{rv} = \frac{1}{C}\sum_{c=1}^{C} \mathbf{y}_{rv}(t_c)\mathbf{y}_{rv}(t_c)^H \quad \cdots(34)$$

Where $\hat{(\cdot)}$ denotes practical measurements. Notice that the number of calculations C must be large enough to ensure an unbiased estimation.

3. DOA estimation:

One of the well-known and efficient algorithms used to estimate the DOA of signals impinging on an antenna array is the Multiple Signal Classification (MUSIC) algorithm [29]. This algorithm exploits the orthonormal signal or noise subspaces of the received signals, calculated from the spectral decomposition of the covariance matrix of the measurements, to estimate the DOAs of the received signals. If the array shown in Fig.1 is made up of all-active (traditional) antennas and receives the same number of signals, the noisy measurements $\mathbf{x}_a(t) \in \mathbb{C}^{Q\times 1}$, with mutual coupling present between the array elements, are given by:

$$\mathbf{x}_a(t) = \mathbf{M}\mathbf{A}(\phi)\mathbf{s}(t) + \mathbf{n}(t) \quad \cdots(35)$$

Where $\mathbf{M}$, $\mathbf{A}(\phi)$, $\mathbf{s}(t)$, and $\mathbf{n}(t)$ are previously defined in Section 2. The covariance matrix, $\mathbf{D}_a \in \mathbb{C}^{Q\times Q}$, is calculated from the expectation $E(\mathbf{x}_a(t)\mathbf{x}_a(t)^H)$, and is given by:

$$\begin{aligned}\mathbf{D}_a &= E(\mathbf{x}_a(t)\mathbf{x}_a(t)^H)\\ &= \mathbf{M}\mathbf{A}(\phi)E(\mathbf{s}(t)\mathbf{s}(t)^H)\mathbf{A}(\phi)^H\mathbf{M}^H + \mathbf{n}(t)\mathbf{n}(t)^H\\ &= \mathbf{M}\mathbf{A}(\phi)\mathbf{S}\mathbf{A}(\phi)^H\mathbf{M}^H + \sigma_a^2\boldsymbol{I}_Q \quad \cdots(36)\end{aligned}$$

Where σ_a^2 is the noise power in the case of an all-active antenna array. The eigenvalue decomposition (EVD) decomposes the covariance matrix of the measurements into two subspaces: the signal subspace ($\boldsymbol{E}_s$) and the noise subspace ($\boldsymbol{E}_n$), as follows:

$$\mathbf{D}_a = \boldsymbol{E}_s\boldsymbol{\Lambda}_s\boldsymbol{E}_s^H + \boldsymbol{E}_n\boldsymbol{\Lambda}_n\boldsymbol{E}_n^H \quad \cdots(37)$$

The elements of the diagonal matrices $\boldsymbol{\Lambda}_s$ and $\boldsymbol{\Lambda}_n$ are the eigenvalues of the signal subspace and noise subspace, respectively. The order of these eigenvalues should be $\Lambda_1 > \Lambda_2 > \cdots > \Lambda_P > \Lambda_{P+1} \approx \Lambda_{P+2} \approx \cdots \approx \Lambda_Q \approx \sigma_a^2$. When the array's vicinity is noiseless, $\Lambda_{P+1} = \Lambda_{P+2} = \cdots = \Lambda_Q = 0$.

In practice, the covariance matrix, $\widehat{\mathbf{D}}_a$, is obtained from:

$$\widehat{\mathbf{D}}_a = \frac{1}{C}\sum_{c=1}^{C} \mathbf{x}_a(t_c)\mathbf{x}_a(t_c)^H \quad \cdots(38)$$

The estimated noise subspace, $\widehat{\boldsymbol{E}}_n$, can be calculated from the EVD of $\widehat{\mathbf{D}}_a$, same as in eq. (37), i.e.:

$$\widehat{\mathbf{D}}_a = \widehat{\boldsymbol{E}}_s\widehat{\boldsymbol{\Lambda}}_s\widehat{\boldsymbol{E}}_s^H + \widehat{\boldsymbol{E}}_n\widehat{\boldsymbol{\Lambda}}_n\widehat{\boldsymbol{E}}_n^H \quad \cdots(39)$$

The cost function of the MUSIC algorithm with the mutual coupling present is [30]:

$$P_{MUSIC}(\phi) = \frac{1}{\boldsymbol{a}^H(\phi)\mathbf{M}^H\widehat{\boldsymbol{E}}_n\widehat{\boldsymbol{E}}_n^H\mathbf{M}\boldsymbol{a}(\phi)} = \frac{1}{\|\widehat{\boldsymbol{E}}_n^H\mathbf{M}\boldsymbol{a}(\phi)\|_2^2} \quad \cdots(40)$$

$\boldsymbol{a}(\phi)$ is the steering vector, which is defined in eq. (4) for every potential direction, and $\|\ \|_2$ is the 2-norm. The MUSIC algorithm detects the DOA of the incoming signals as peaks when the quadratic function of the denominator approximately equals to zero (i.e., when $\mathbf{M}\boldsymbol{a}(\phi_p)$ is orthogonal to $\widehat{\boldsymbol{E}}_n^H$). Table 1 summarizes the DOA estimation steps using the MUSIC algorithm.

Table (1): The MUSIC algorithm.

DOA estimation of signals received by an all-active ULA antenna array using the MUSIC algorithm.
Step one: Collect the measurements, $\hat{\mathbf{x}}_a(t_c)$, from the antenna array.
Step two: Calculate the covariance matrix, $\widehat{\mathbf{D}}_a$, as in eq. (38).
Step three: Calculate the EVD of $\widehat{\mathbf{D}}_a$.
Step four: Estimate the noise subspace, $\widehat{\boldsymbol{E}}_n$, from the previous step by selecting the columns accompanied by the eigenvalues $\Lambda_{P+1} \approx \Lambda_{P+2} \approx \cdots \approx \Lambda_Q \approx \sigma_a^2$.
Step five: Use the estimated noise subspace in the cost function of the MUSIC algorithm of eq. (40) to estimate the DOAs of the received signals.

To estimate the DOAs of signals impinging on a SASPA-ULA array, the EVD of the covariance matrix, $\breve{\mathbf{D}}$, of the SASPA measurement, which is calculated from eq. (33) should be determined, i.e.:

$$\breve{\mathbf{D}} = \breve{\boldsymbol{E}}_s\breve{\boldsymbol{\Lambda}}_s\breve{\boldsymbol{E}}_s^H + \breve{\boldsymbol{E}}_n\breve{\boldsymbol{\Lambda}}_n\breve{\boldsymbol{E}}_n^H \quad \cdots(41)$$

The $\breve{\boldsymbol{E}}_s$ and $\breve{\boldsymbol{E}}_n$ represent the signal and noise subspaces of a SASPA's measurements, respectively. The entries of the diagonal matrices $\breve{\boldsymbol{\Lambda}}_s$ and $\breve{\boldsymbol{\Lambda}}_n$ are the signal and noise eigenvalues, respectively. Thus, to estimate the DOAs of the signals received by a SASPA array, the MUSIC cost function in eq. (40) should be updated to:

$$P_{MUSIC-SASPA}(\phi) = \frac{1}{\mathbf{m}^{(1)H}\mathbf{K}(\phi)^T\breve{\boldsymbol{E}}_n\breve{\boldsymbol{E}}_n^H\mathbf{K}(\phi)\mathbf{m}^{(1)}} = \frac{1}{\|\breve{\boldsymbol{E}}_n^H\mathbf{K}(\phi)\mathbf{m}^{(1)}\|_2^2} \quad \cdots(42)$$

A real-valued noise subspace, $\breve{\boldsymbol{E}}_{n,rv}$, can be determined from the EVD of $\mathbf{D}_{rv}$, defined in eq. (34), i.e.:

$$\breve{\mathbf{D}}_{rv} = \breve{\boldsymbol{E}}_{s,rv}\breve{\boldsymbol{\Lambda}}_{s,,rv}\breve{\boldsymbol{E}}_{s,,rv}^H + \breve{\boldsymbol{E}}_{n,rv}\breve{\boldsymbol{\Lambda}}_{n,,rv}\breve{\boldsymbol{E}}_{n,,rv}^H \quad \cdots(43)$$

will contribute to further improvement in the resolution of DOA estimation when used in the cost function of eq. (42) instead of $\breve{\boldsymbol{E}}_n$. Additionally, further reductions in computational complexity will be achieved, as will be shown in the simulation in the next section. Table 2 outlines the steps for DOA estimation using a SASPA array in conjunction with the MUSIC algorithm.

Table 2. The Proposed Method

DOA estimation of signals received by a SASPA-ULA array using the MUSIC algorithm.
Step one: Collect the measurements $\mathbf{x}_{SASPA-ULA}(t)$
Step two: Calculate $\mathbf{y}_{SASPA-ULA1}(t)$
Step three: Calculate $\mathbf{y}_{SASPA-ULA2}(t)$.
Step four: Estimate the covariance matrices of the measurements: $\mathbf{y}(t) = [\mathbf{y}_{SASPA-ULA2}(t) \quad \mathbf{y}_{SASPA-ULA2}(t)]^T$. and $\mathbf{y}_{rv}(t) = (\mathbf{y}(t) + \mathbf{y}(t)^*)/2$
Step five: Estimate the noise subspaces, $\breve{\boldsymbol{E}}_n$ and $\breve{\boldsymbol{E}}_{n,rv}$ from the previous step.

Step six: Use these subspaces to estimate the DOAs of the received signals using the updated MUSIC cost function of eq. 42.

4. Simulated Results and Discussion

This section presents the outcomes of various simulated scenarios carried out when a SASPA array receives multiple signals. The simulations, conducted using MATLAB, demonstrate the effectiveness of SASPA arrays in terms of DOA estimation resolution and processing time compared to conventional all-active antenna arrays. Fig. 2 depicts, using the MUSIC algorithm, the capability of a 6-element SASPA-ULA array when receiving two signals coming from the directions $\phi_1 = 60^\circ$ and $\phi_2 = 62^\circ$. The elements of the array are half-wave dipole antennas with an inter-element spacing of $r = 0.15\lambda$ between them. The signals were received with a signal-to-noise ratio (SNR) of 0 dB. Fig. 2a shows that the SASPA-ULA array has significantly improved the DOA estimation with very high resolution. A superior resolution of DOA estimation has been achieved when the real-valued noise subspace, $\breve{\boldsymbol{E}}_{n,rv}$, calculated from eq. (43), is used in the MUSIC cost function. However, the antenna array with all-active antenna elements and the same geometry failed to estimate the underlying DOAs, as shown in Fig. 2c. Fig. 3 illustrates that the SASPA-ULA array performs efficiently, as previously observed, when the signals come from end-fire directions. The signals in this simulation were assumed to come from the critical directions $\phi_1 = 20^\circ$ and $\phi_2 = 23^\circ$. However, it was required that the signals be received with a higher SNR of 10 dB. The resolution of DOA estimation for these signals was very high. Using $\breve{\boldsymbol{E}}_{n,rv}$ has resulted in much better resolution than using $\breve{\boldsymbol{E}}_n$ in the MUSIC cost function of eq. (42). The two scenarios illustrated demonstrate that SASPA arrays can estimate incoming signals, regardless of their proximity, directions, low SNR, and the compact size of the array. The all-active array was again disabled to accurately determine the DOAs of the received signals. Fig.4 illustrates the DOA estimation of four signals coming from the directions $\phi_1 = 50^\circ$, $\phi_2 = 52^\circ$, $\phi_3 = 80^\circ$, and $\phi_4 = 82^\circ$. All of these signals were received with an SNR of 0 dB. The figure clearly shows that they can be successfully detected with very high resolution when a SASPA-ULA array constructed from ten half-wave dipoles is utilized, while an all-active ULA antenna array with the same geometry failed to do so. Another set of simulations has been conducted to show the effectiveness of the real-valued steering matrix produced by the SASPA array when the processing time of DOA estimation is considered. The simulations compare SASPA and all-active arrays when the MUSIC cost function is used. Figs. 5 to 7 show how much time is spent by the SASPA arrays and the analogous all-active antenna array when calculating the DOAs from the MUSIC cost function for the three scenarios of Figs. 2 to 4. The figures clearly demonstrate that using the noise subspace of the SASPA array, $\breve{\boldsymbol{E}}_n$, took much less time (one-half on average) than using the all-active noise subspace, $\widehat{\boldsymbol{E}}_n$. The processing time of the MUSIC cost function is further decreased (approximately one-third) when using the real-valued noise subspace $\breve{\boldsymbol{E}}_{n,rv}$ calculated from eq. (43) along with the real-valued search steering vector in eq. (42). These results validate that the DOA estimation with a SASPA-ULA is faster than when employing an all-active ULA antenna array, irrespective of the conditions of the scenarios mentioned above.

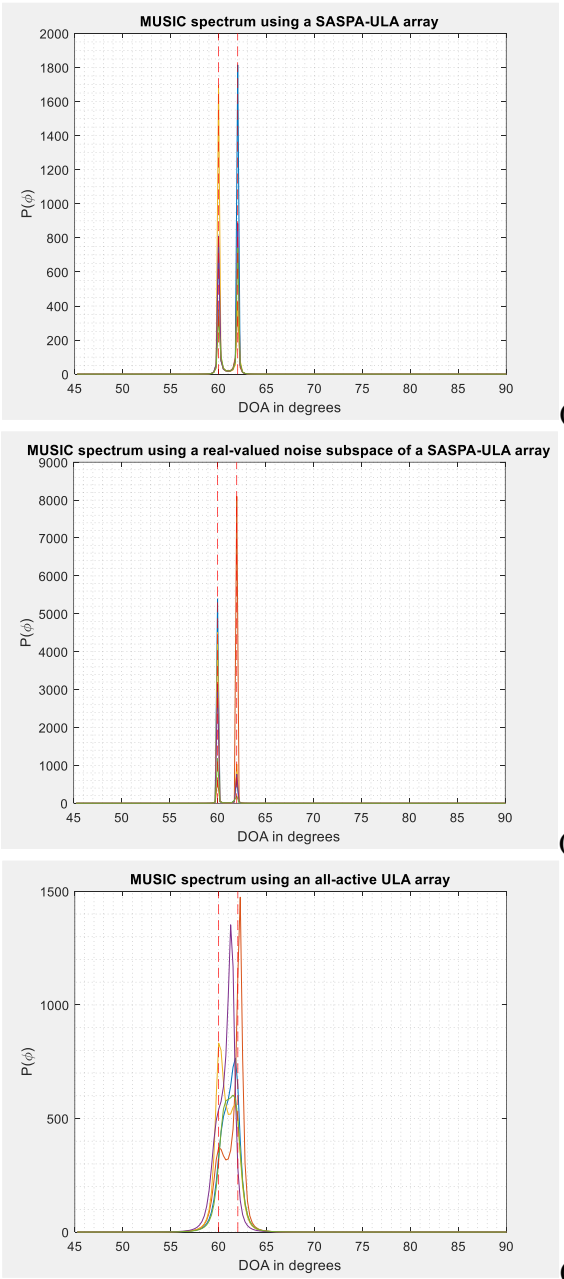

Figure 2. MUSIC spectrums for two signals coming from the directions $\phi_1 = 60^\circ$ and $\phi_2 = 62^\circ$ and impinging on a six-element half-wave dipole antenna array. The inter-element spacing is $r = 0.15\lambda$ and the signals are received with (SNR) of 0 dB, **a)** a SASPA-ULA array, **b)** using a real-valued noise subspace of a SASPA-ULA array, **c)** an all-active ULA array.

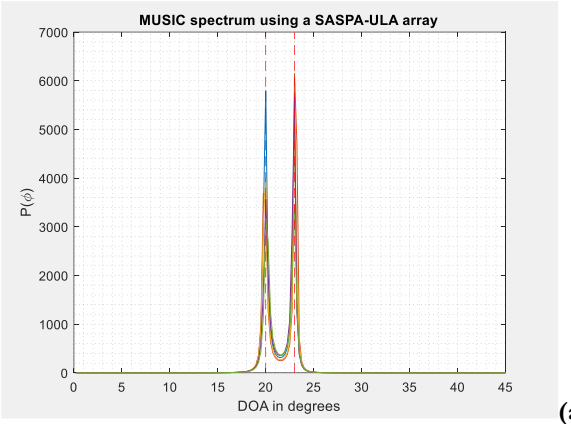

(a)

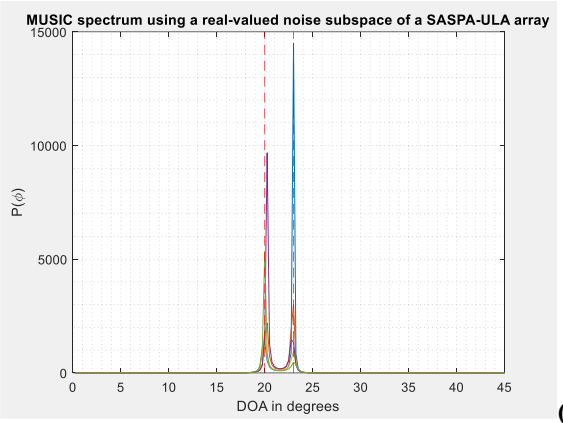

(b)

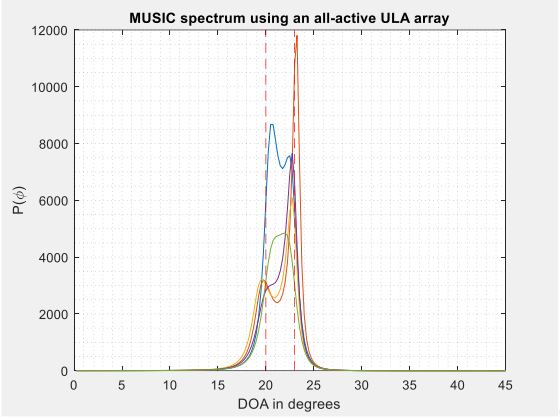

(c)

Figure 3. MUSIC spectrums for two signals coming from the directions $\phi_1 = 20^{\circ}$ and $\phi_2 = 23^{\circ}$ and impinging on a six-element half-wave dipole antenna array. The inter-element spacing is $r = 0.15\lambda$ and the signals are received with (SNR) of 0 dB, **a)** a SASPA-ULA array, **b)** using a real-valued noise subspace of a SASPA-ULA array, **c)** an all-active ULA array.

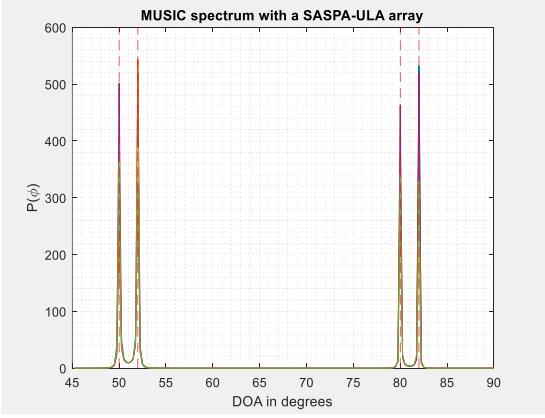

(a)

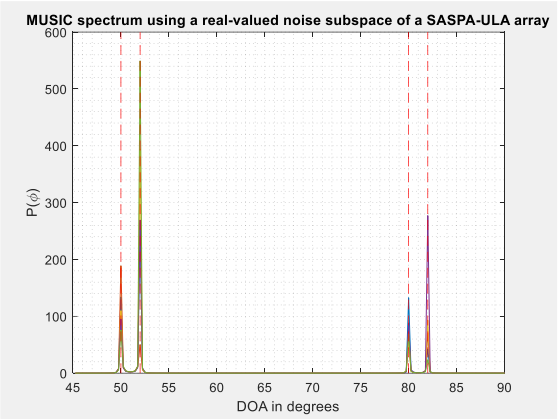

(b)

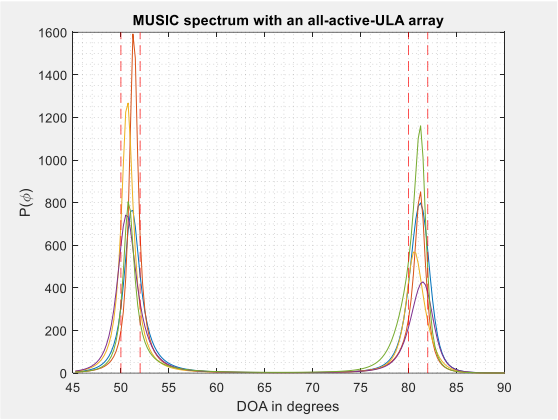

(c)

Figure 4. MUSIC spectrums for four signals coming from the directions $\phi_1 = 50^{\circ}, \phi_2 = 52^{\circ}\ \phi_3 = 80^{\circ}, \phi_4 = 82^{\circ}$ and impinging on a ten-element half-wave dipole antenna array. The inter-element spacing is $r = 0.15\lambda$ and the signals are received with (SNR) of 0 dB, **a)** a SASPA-ULA array, **b)** using a real-valued noise subspace of a SASPA-ULA array, **c)** an all-active ULA array.

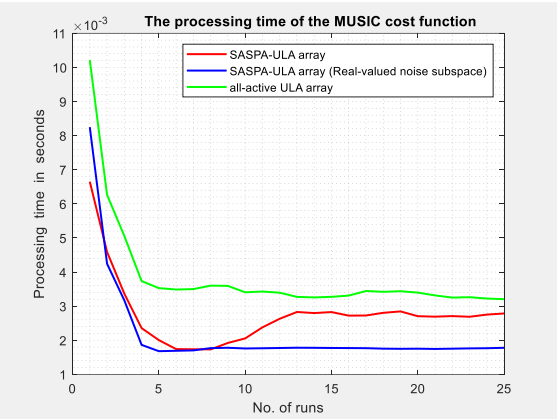

Figure 5. The processing time of the MUSIC cost function for the scenario in Fig. (2).

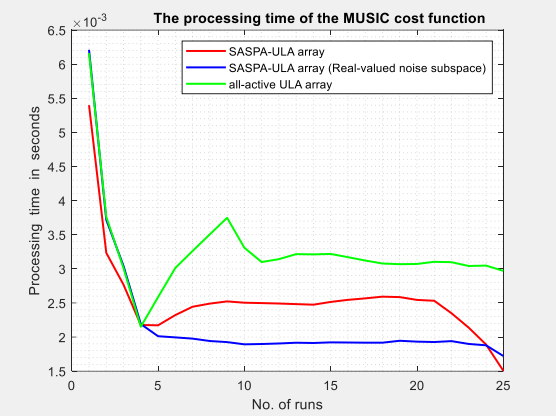

Figure 6. The processing time of the MUSIC cost function for the scenario in Fig. (3).

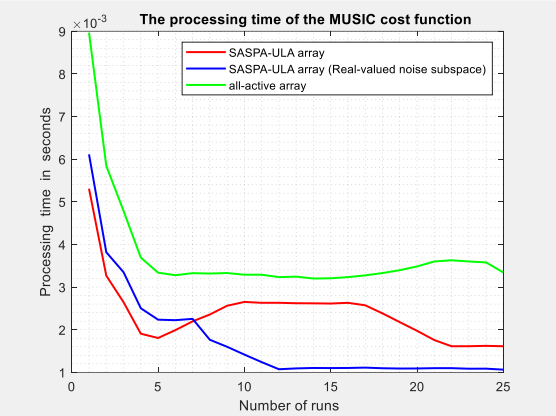

Figure 7. The processing time of the MUSIC cost function for the scenario in Fig. (4).

5. Conclusions

The effectiveness of the real-valued steering matrix in the signal data generated by a receiving SASPA-ULA array is investigated in this research. Due to its beneficial inherent characteristics, SASPA-ULA arrays provide a steering matrix with real values after a simple arrangement of the array measurements and without applying any unitary transformation. Accordingly, the resultant real-valued noise subspace, which is calculated from the covariance matrix of the SASPA-ULA's measurements, along with the real valued steering vector, significantly results in very high resolution of DOA estimation in conjunction with the MUSIC algorithm. In addition to being estimated with very high resolution compared to all-active antenna arrays, the processing time of DOA estimation is meaningfully reduced due to a reduction in required computations. Several simulations in this work showed that a SASPA-ULA possesses the ability to estimate DOAs of signals impinging on it with very high resolution despite the array size being very compact and the signals being received from different directions, with low SNR, and closely spaced. Also, the simulations showed that the processing of DOA estimation with a SASPA-ULA is much faster than that of a conventional ULA with an all-active antenna array. The simulations demonstrated in this research that when implementing the noise subspaces calculated from the measurements of SASPA arrays, the processing time for DOA estimation has been reduced to one-half and one-third of the processing time taken by all-active antenna arrays. These benefits are crucial for systems designed for next-generation communications, where huge data exchanges with very high speed and secure transfers in very dense areas are compulsory.

6. References

[1] Y. Tian, R. Wang, H. Chen, Y. Qin, and M. Jin, "Real-valued DOA estimation utilizing enhanced covariance matrix with unknown mutual coupling," IEEE Commun. Lett., vol. 26, no. 4, pp. 912-916, 2022.
https://doi.org/10.1109/LCOMM.2022.3148260

[2] T.-H. Sang, F.-T. Chien, C.-C. Chang, K.-Y. Tseng, B.-S. Wang, and J.-I. Guo, "DoA estimation for FMCW radar by 3D-CNN," Sensors, vol. 21, no. 16, p. 5319, 2021.
https://doi.org/10.3390/s21165319

[3] M. A. G. Al-Sadoon et al., "Low complexity antenna array DOA system for localization applications," in Proc. 6th Int. Conf. Wireless Netw. Mobile Commun. (WINCOM), Oct. 2018, pp. 1-5.
https://doi.org/10.1109/WINCOM.2018.8629656

[4] T. Troccoli, J. Pirskanen, A. Ometov, J. Nurmi, and V. Kaseva, "Fast real-world implementation of a direction of arrival method for constrained embedded IoT devices," in Proc. Int. Conf. Internet Things (IoT 2022), 2023, pp. 1-8.
https://doi.org/10.1145/3567445.3567446

[5] M. Hasib, S. Kandeepan, W. S. T. Rowe, and A. Al-Hourani, "Direction-of-arrival (DoA) estimation performance for satellite applications in a multipath environment with Rician fading and spatial correlation," Sensors, vol. 23, no. 12, p. 5458, 2023.
https://doi.org/10.3390/s23125458

[6] S. Kulkarni, A. Thakur, S. Soni, A. Hiwale, M. Belsare, and D. A. Raj, "A comprehensive review of direction of arrival (DoA) estimation techniques and algorithms," J. Electron. Electr. Eng., vol. 4, pp. 1-50, Feb. 2025.
https://doi.org/10.37256/jeee.4120255708

[7] R. Varzandeh, S. Doclo, and V. Hohmann, "Improving multi-talker binaural DOA estimation by combining periodicity and spatial features in convolutional neural networks," EURASIP J. Audio Speech Music Process., vol. 2025, no. 1, p. 5, Feb. 2025.
https://doi.org/10.1186/s13636-025-00392-8

[8] Y. Lu, H. Guan, K. Yang, T. Peng, C. Wen, and X. Li, "Improving the accuracy of direction of arrival estimation with multiple signal inputs using deep learning," Sensors, vol. 24, no. 10, p. 2971, 2024.
https://doi.org/10.3390/s24102971

[9] Y. Jeong, H. Kim, B.-S. Kim, and H. Choo, "Avoidance of co-channel interference using switched parasitic array antenna in femtocell networks," in Comput. Sci. Appl. - ICCSA 2010, Berlin, Heidelberg: Springer, 2010, pp. 158-167.
https://doi.org/10.1007/978-3-642-12179-1_15

[10] A. A. D. Amico and M. Morelli, "Joint channel and DOA estimation for multicarrier CDMA uplink transmissions," IEEE Trans. Veh. Technol., vol. 58, no. 1, pp. 116-125, 2009.
https://doi.org/10.1109/TVT.2008.921624

[11] P. K. Pal and R. S. Sherratt, "MIMO channel capacity and configuration selection for switched parasitic antennas," ETRI J., vol. 40, no. 2, pp. 197-206, 2018.

https://doi.org/10.4218/etrij.2017-0071
[12] L. Kulas, "Simple 2-D direction-of-arrival estimation using ESPAR antenna," IEEE Antennas Wireless Propag. Lett., vol. PP, pp. 1-1, Jul. 2017.
https://doi.org/10.1109/LAWP.2017.2728322
[13] H. Cao and Q. Liu, "Accurate DOA estimation based on real-valued singular value decomposition," in Proc. IEEE Int. Conf. Signal, Inf. Data Process. (ICSIDP), 2019.
https://doi.org/10.1109/ICSIDP47821.2019.9172819
[14] T. Chen, H. Wu, and Z. Zhongkai, "The real-valued sparse direction of arrival (DOA) estimation based on the Khatri-Rao product," Sensors, vol. 16, p. 693, May 2016.
https://doi.org/10.3390/s16050693
[15] J. Dai, W. Xu, and D. Zhao, "Real-valued DOA estimation for uniform linear array with unknown mutual coupling," Signal Process., vol. 92, no. 9, pp. 2056-2065, 2012.
https://doi.org/10.1016/j.sigpro.2012.01.017
[16] J. Li, F. Wang, and D. Jiang, "DOA estimation based on real-valued cross correlation matrix of coprime arrays," Sensors, vol. 17, p. 638, Mar. 2017.
https://doi.org/10.3390/s17030638
[17] L. Li, X. Wang, J. Shi, and X. Lan, "Real-valued weighted subspace fitting algorithm for DOA estimation with block sparse recovery," Math. Probl. Eng., vol. 2023, no. 1, p. 7199603, 2023.
https://doi.org/10.1155/2023/7199603
[18] T. Ma, M. Yang, and Y. Chen, "A real-valued high-resolution coherent DOA estimation method with unknown source number," Digit. Signal Process., vol. 167, p. 105408, 2025.
https://doi.org/10.1016/j.dsp.2025.105408
[19] X.-T. Meng, B.-X. Cao, F.-G. Yan, M. Greco, F. Gini, and Y. Zhang, "Real-valued MUSIC for efficient direction of arrival estimation with arbitrary arrays: mirror suppression and resolution improvement," Signal Process., vol. 202, p. 108766, 2023.
https://doi.org/10.1016/j.sigpro.2022.108766
[20] W. Si, P. Zhao, Z. Qu, and Y. Wang, "Real-valued DOA estimation for a mixture of uncorrelated and coherent sources via unitary transformation," Digit. Signal Process., vol. 58, pp. 102-114, 2016.
https://doi.org/10.1016/j.dsp.2016.07.024
[21] F. Sun, Q. Wu, P. Lan, G. Ding, and L. Chen, "Real-valued DOA estimation with unknown number of sources via reweighted nuclear norm minimization," Signal Process., vol. 148, pp. 48-55, 2018.
https://doi.org/10.1016/j.sigpro.2018.02.014
[22] F.-G. Yan, J. Wang, S. Liu, Y. Shen, and M. Jin, "Reduced-complexity direction of arrival estimation using real-valued computation with arbitrary array configurations," Int. J. Antennas Propag., vol. 2018, no. 1, p. 3284619, 2018.
https://doi.org/10.1155/2018/3284619
[23] D.-S. Yang, F. Chen, and S.-Q. Mo, "A novel real-valued DOA algorithm based on eigenvalue," Sensors, vol. 20, no. 1, p. 40, 2020.
https://doi.org/10.3390/s20010040
[24] C. A. Balanis, Antenna Theory: Analysis and Design, 4th ed. Hoboken, NJ, USA: Wiley, 2016.
[25] Z. Liu, Z. Huang, F. Wang, and Y. Zhou, "DOA estimation with uniform linear arrays in the presence of mutual coupling via blind calibration," Signal Process., vol. 89, no. 7, pp. 1446-1456, 2009.
https://doi.org/10.1016/j.sigpro.2009.01.017
[26] H.-J. Kim, "On the distribution and its properties of the sum of a normal and a doubly truncated normal," Commun. Stat. Appl. Methods, vol. 13, pp. 255-266, 2006.
https://doi.org/10.5351/CKSS.2006.13.2.255
[27] Wikipedia Contributors, "Sum of normally distributed random variables," Wikipedia, Wikimedia Foundation, Nov. 2025. [Online]. Available: en.wikipedia.org. Accessed: Dec. 8, 2025.
[28] W.-H. S. Y. Hardy, Matrix Calculus and Kronecker Product: A Practical Approach to Linear and Multilinear Algebra, 2nd ed. Singapore: World Scientific Publ. Co. Pte Ltd, 2011.
[29] R. Schmidt, "Multiple emitter location and signal parameter estimation," IEEE Trans. Antennas Propag., vol. 34, no. 3, pp. 276-280, 1986.
https://doi.org/10.1109/TAP.1986.1143830
[30] C. S. Ateşavcı, Y. Bahadırlar, and S. Aldırmaz-Çolak, "DoA estimation in the presence of mutual coupling using root-MUSIC algorithm," in Proc. 8th Int. Conf. Electr. Electron. Eng. (ICEEE), 2021, pp. 292-298.
https://doi.org/10.1109/ICEEE52452.2021.9415938